NUCL SCI TECH (2019) 30:91
https://doi.org/10.1007/s41365-019-0623-1

Physical studies of minor actinide transmutation in the accelerator-driven subcritical system

Hai-Yan Meng[1] · Yong-Wei Yang[1,2] · Ze-Long Zhao[1,2] · Qing-Yu Gao[1,2] · Yu-Cui Gao[1]

Received: 16 October 2018 / Revised: 10 January 2019 / Accepted: 31 January 2019 / Published online: 15 May 2019

Abstract The accelerator-driven subcritical system (ADS) with a hard neutron energy spectrum was used to study transmutation of minor actinides (MAs). The aim of the study was to improve the efficiency of MA transmutation while ensuring that variations in the effective multiplication factor (k_{eff}) remained within safe margins during reactor operation. All calculations were completed using code COUPLE3.0. The subcritical reactor was operated at a thermal power level of 800 MW, and a mixture of mononitrides of MAs and plutonium (Pu) was used as fuel. Zirconium nitride (ZrN) was used as an inert matrix in the fuel elements. The initial mass composition in terms of weight percentages in the heavy metal component (IHM) was 30.6% Pu/IHM and 69.4% MA/IHM. To verify the feasibility of this MA loading scheme, variations in k_{eff}, the amplification factor of the core, maximum power density and the content of MAs and Pu were calculated over six refueling cycles. Each cycle was of 600 days duration, and therefore, there were 3600 effective full power days. Results demonstrated that the effective transmutation support ratio of MAs was approximately 28, and the ADS was able to efficiently transmute MAs. The changes in other physical parameters were also within their normal ranges. It is concluded that the proposed MA transmutation scheme for an ADS core is reasonable.

Keywords ADS · COUPLE3.0 · MA · Transmutation · Subcritical reactor

1 Introduction

High-level radioactive waste (HLW) arising from the spent fuel of nuclear power plants is increasing with the development of nuclear energy. Given the nature of HLW, in particular that it contains high concentrations of long-lived fission products (LLFPs), Pu and minor actinides (MAs), its disposal has become an urgent problem facing the nuclear industry [1]. At present, one of the most promising methods for dealing with HLW is partition and transmutation (P&T) [2]. The accelerator-driven subcritical system (ADS) is a facility that can be used as a neutron source for transmuting MAs. The ADS is a hybrid system that comprises a high intensity proton accelerator, a spallation target and a subcritical reactor. Protons are injected into the spallation target to produce neutrons that then drive the subcritical reactor core. The target is made of heavy metals (HMs) in solid or liquid state. Compared to a traditional critical reactor, the subcritical reactor of an ADS has a higher-energy neutron energy spectrum, higher flux and wider energy distribution, which can be used to transmute MAs and LLFPs [3]. The reactivity margin of an ADS to prompt criticality can be increased by an extra margin that does not depend on delayed neutrons. This enables the safe operation of a core with degraded characteristics, for example, if pure MA burners are used, excess reactivity can be eliminated, allowing the design of

This work was supported by the Strategic Priority Research Program of The Chinese Academy of Sciences (No. XDA21010202).

✉ Yong-Wei Yang
yangyongwei@impcas.ac.cn

[1] Institute of Modern Physics, Chinese Academy of Sciences, Lanzhou 730000, China

[2] School of Nuclear Science and Technology, University of Chinese Academy of Sciences, Beijing 100049, China

cores with a reduced potential for reactivity-induced accidents [4]. The ADS has been studied in many nations, for example, the initial accelerator-driven system (CiADS) program in China [5]; the multipurpose accelerator-driven system for research and development (MYRRHA) in Belgium [6]; the OMEGA program and the high intensity proton accelerator project in Japan (J-PARC) [7, 8]; and the research program on separation–incineration (SPIN) in France [9].

In this study, the initial design parameters were as follows: (1) Pu and MA content of fuel; (2) the inert matrix materials; (3) type of coolant; (4) type of cladding and its thickness; (5) height, material and structure of shielding; (6) reflector height and components; (7) core activity zone height; (8) type of fuel pellet; (9) fuel component structure; and (10) proton beam energy. The search parameters were initial Pu loading, the type of inert matrix and the number of fuel assemblies.

Change in the effective multiplication factor (k_{eff}) are important in the design of an ADS core [10]. The purpose of this study was to establish those core design parameters that will give rise to little k_{eff} variation within 500 days of full power operation. Another significant aspect of ADS design is achieving a low transmutation supplier-to-burner support ratio [11]. In order to improve the characteristics of MA transmutation, the impacts of initial loading of MAs on the efficiency of MA transmutation were investigated. In Sect. 2, the method of burnup calculation and fuel design are introduced. In Sect. 3, fuel burn up characteristic parameters are determined and analyzed. In Sect. 4, the results of calculations and analyses for long-period refueling fuel burnup of an ADS are presented.

2 Computational methods and software

2.1 Calculation code

The code COUPLE3.0 [12] was used for all calculations. This code is a three-dimensional transport-burnup simulation program developed by the Institute of Modern Physics, Chinese Academy of Sciences. The transport calculation of code COUPLE3.0 was performed by Monte Carlo code MCNPX2.7 [13], and the burnup calculation was performed by ORIGEN2.1 [14]. There are some similar coupling transport codes, such as MONTEBURNS [15] and ALEPH [16]. The code COUPLE3.0 uses the cross section library ENDF/B-VII.0. In studying the loading scheme for MA transmutation, the proton radiation module, the critical calculation module and the data postprocessing module were used. First, the proton radiation module was used: The total task file "task.inp" had to be prepared, which gives global calculation parameters, including the simulation type, core thermal power and effective full power days (EFPDs). After the calculation of proton irradiation was completed, the critical calculation module was used: the "source.inp" file was written, where k_{code} and k_{src} were given, k_{eff} of each burnup step had to be calculated, and changes in k_{eff} during the operation of the ADS were observed [13].

In order to maintain the stability of core k_{eff} and the core amplification factor during the entire fuel cycle, all or part of the fuel assembly needed to be refueled, the timing of which reflected the degree of burnup. All of this was completed using code COUPLE3.0.

2.2 Fuel for MA transmutation

For the core fuel, a mixture of mono-nitrides of MAs and Pu was used [17]. Zirconium nitride (ZrN) was also used in the fuel elements as an inert matrix. Nitrogen with N-15 enriched (100%) was used for (Pu, MA)-nitride and ZrN. Nitrides have suitable physical properties, and Pu and MAs do not have resonance cross sections in the fast neutron energy range (Fig. 1) [18]. Nitrides can also be made into a cylindrical shape, which reduces the space self-shielding effect. Moreover, in the fast neutron region, the capture cross sections of MAs decrease with increased neutron energy, whereas the fission cross section increases with increased neutron energy and the capture-to-fission ratios increase. Lead–bismuth was used as the coolant to reduce the moderating effect of neutrons, and this ensured that a hard neutron energy spectrum was maintained in the active core region that would be more conducive to the transmutation of MAs.

The production and isotopic composition of MAs and Pu from their originating the pressurized water reactor (PWR) are shown in Tables 1 and 2; the power of the PWR was 1 GWe, equivalent to 3.3 GWth. The operation time was

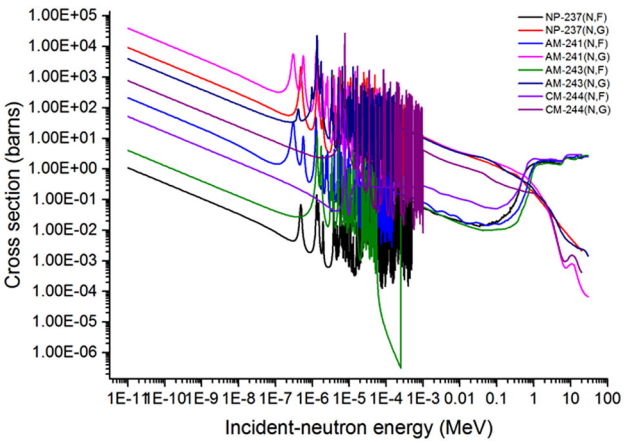

Fig. 1 (Color online) Capture and fission cross section of a selection of MAs

Table 1 Isotopic composition ratio of MAs [19]

Nuclide	$T_{1/2}$ (a)	m (kg Gwe^{-1} a^{-1})	Mass composition (wt%)
^{237}Np	2.144×10^{6}	13.38	56.2
^{241}Am	432.6	6.28	26.4
^{243}Am	7364	2.86	12.0
^{243}Cm	29.1	7.14×10^{-3}	0.03
^{244}Cm	18.1	1.22	5.11
^{245}Cm	8423	6.67×10^{-2}	0.28
Total		23.81	

Table 2 Isotopic composition ratio of Pu [20]

Isotope	$T_{1/2}$ (a)	Mass composition (wt%)
^{238}Pu	87.7	1.81
^{239}Pu	2.411×10^{4}	59.14
^{240}Pu	6561	22.96
^{241}P	14.329	12.13
^{242}Pu	3.75×10^{5}	3.96

1 year, the fuel burnup depth was 33 GWd/t, and the cooling time was 3 years [19]. The specific ability for MA production (SAMAP) was 23.81/3.3 $\approx$ 7.2 kg Gwt^{-1} a^{-1}.

2.3 Transmutation effectiveness of MAs

Transmutation performance is an important parameter when choosing an appropriate MA loading scheme for an ADS core. In this paper, direct fission of MAs and the fission of secondary heavy nuclei generated by MAs were defined as effective transmutation. ΔM_{MA} was defined as the gross mass change in the initial MAs; $\Delta M_{\mathrm{MA}\to\mathrm{Pu}\to\mathrm{U}}$ as the mass change in the initial MAs transmuted to uranium isotopes; $\Delta M_{\mathrm{MA}\to\mathrm{Pu}}$ as the mass change in the initial MAs transmuted to Pu isotopes; $\Delta M_{\mathrm{MA}\to\mathrm{TRMA}}$ as the mass change in the initial MAs transmuted to higher-Z MAs; and ΔM_{MA} (EFF) as the net change in the initial MAs due to their fission reactions and those of their daughter nuclides. The formula for calculating MA effective transmutation mass is as follows:

$$\Delta M_{\mathrm{MA}}(\mathrm{EFF}) = \Delta M_{\mathrm{MA}} + \Delta M_{\mathrm{MA}\to\mathrm{Pu}} + \Delta M_{\mathrm{MA}\to\mathrm{Pu}\to\mathrm{U}} + \Delta M_{\mathrm{MA}\to\mathrm{TRMA}}.$$

3 Search for core design scheme

The search for the ADS was conducted using the total loading mass of Pu, the number of fuel assemblies and the total amount of inert matrix. However, there were some fixed parameters in the ADS, and they are listed in Table 3. The calculation flow for the parametric search is shown in Fig. 2.

The core thermal power was 800 MW and burnup history was 500 EFPDs. In this study, the MA inventory was fixed at 3000 kg of initial core. For all cases, the initial core k_{eff} was set to 0.97, whereas the parametric survey and fuel burnup analysis were carried out by adjusting the number of fuel assemblies, the amount of Pu of the initial loading and the total amount of inert matrix. The main purpose of the parameter search was to define the ADS core whose k_{eff} decreased over the 500 EFPDs and was between 0.9590 and 0.9705. After the fuel loading scheme was determined, the core burnup was calculated over the longer period of 3600 EFPDs.

Following a series of calculations, five cases of different Pu loadings were derived and the parameters of each scheme are shown in Table 4.

From the results of the search for a core design scheme, the following conclusions applicable to all five cases were drawn:

1. With the initial loading amount of MAs and Pu and the loading amount of inert matrix fixed, the more fuel assemblies in the core and the larger the core volume, the smaller the fuel density and the smaller the core k_{eff} in the initial state.
2. With the initial loading of MAs and Pu fixed, the percentage of inert matrix increased and the fuel density increased, while the core structure of the ADS remained unchanged. The larger the percentage of inert matrix, the smaller the k_{eff}.
3. With the number of fuel components and MA initial loading fixed, the heavy metals (HMs) increased with the increase in Pu initial loading. In order to make the initial k_{eff} of the ADS reach 0.97, the inert matrix must be increased.

The burnup calculation of every case was performed by code COUPLE3.0. The change in k_{eff} over 500 EFPDs was obtained and is shown in Fig. 3.

Figure 3 shows that the k_{eff} of cases 1 to 4 decreased with the increase in burnup time, and the higher the initial loading of Pu (MA 3000 kg), the greater the change in k_{eff}

Table 3 Parameters of ADS

Parameter	Value	Parameter	Value
Beam proton energy (GeV)	1.5	Beam diameter (cm)	20
Thermal power of core (MW)	800	Reflector	SS316L stainless steel
Fuel pellet radius (cm)	0.375	Reflector single rod radius (cm)	0.7
Fuel	(Pu, MA)N + ZrN	Reflector height (cm)	19
Gas thickness (cm)	0.035	Shielding	B_4C
Active region length (cm)	100	Shield single bar radius (cm)	0.7
Cladding thickness (cm)	0.055	Shield height (cm)	9
Target material	LBE	Cladding of fuel rod	316Ti
Target outer wall, beam tube	T91 alloy	Lead–bismuth channels per fuel assembly	6
Fuel rods per fuel assembly	265		

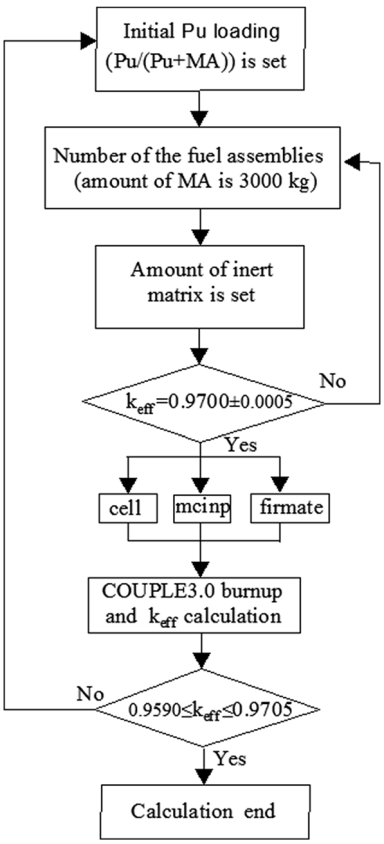

Fig. 2 Calculation flow for the parametric survey calculations

over the consumption time. In contrast, the k_{eff} of the case defined as CASE 5 increased during the burnup history. The reason for this trend is that the percentage of MA loading was too high, the k_{eff} increased with the increase in fuel consumption time, and the k_{eff} increased up to the end of the 500 days cycle. Hence the percentage of MA to HM should be limited to an appropriate value. The ADS system met the calculation requirements when the initial Pu was 30.6% of the initial mass composition in the heavy metal component (IHM) and the loading of the inert matrix was 63.69% IHM. The final solution was therefore found to be CASE 4.

4 Burnup analysis of subcritical core

CASE 4 represented the subcritical reactor core shown in Fig. 4. It consisted mainly of four zones including the target fuel, reflector and shielding assemblies and lead–bismuth eutectic (LBE).

The initial k_{eff} of the ADS core was 0.97009, and the reactivity was − 3083 pcm. The entire core consisted of 78 fuel assemblies, 36 reflector assemblies and 90 shielding layer assemblies. Each fuel assembly contained 265 fuel elements and 6 lead–bismuth channels. In the calculation of long burnup period, 600 EFPDs was a burnup cycle and the total burnup time was 3600 EFPDs. In code COUPLE3.0, the fuel assembly were numbered as shown in Fig. 5.

Table 5 shows the material numbers (1001–1045) of each of the fuel assemblies used in different burnup cycles. In the initial state, each labeled fuel assembly had a corresponding fuel material number. After operation over the first 600 EFPDs, fuel material numbers 1001 to 1006 inclusive in the inner ring fuel assemblies were moved outside the core; 1007 to 1013 inclusive, which had been irradiated for 600 EFPDs in the outer ring fuel assemblies, were relocated to the inner ring regions; and new fuel material numbers 1014 to 1019 inclusive were moved to the outer ring region. The burnup analysis was carried out in this way for six fuel cycles.

The changes in total mass of Pu and mass ratio of Pu to heavy metal (HM) over 3600 EFPDs are shown in Fig. 6a, and changes in total mass of MAs and mass ratio of MAs to

Table 4 Parameters of different initial Pu loading cases

Parameter	Case 1	Case 2	Case 3	Case 4	Case 5
Initial Pu loading in HMs (wt%)	35	32	31	30.6	30
Fuel loading	–	–	–	–	–
Total heavy metal inventory (kg)	4615	4412	4348	4323	4286
Initial MA inventory (kg)	3000	3000	3000	3000	3000
Inert matrix in all fuel (wt%)	64.5	66.6	64.65	63.69	62.335
Fuel assembly number	108	78	78	78	78
The initial mass composition of the fuel element (wt%)	–	–	–	–	–
PU	11.7	10.0	10.3	10.5	10.6
MA	21.7	21.4	23.0	23.7	24.8
Zr	55.4	57.2	55.5	54.7	53.6
N	11.2	11.4	11.2	11.1	11.0
Initial beam power (MW)	13.94	12.72	14.42	15.68	17.22
Initial k_{eff}	0.970	0.970	0.970	0.970	0.970

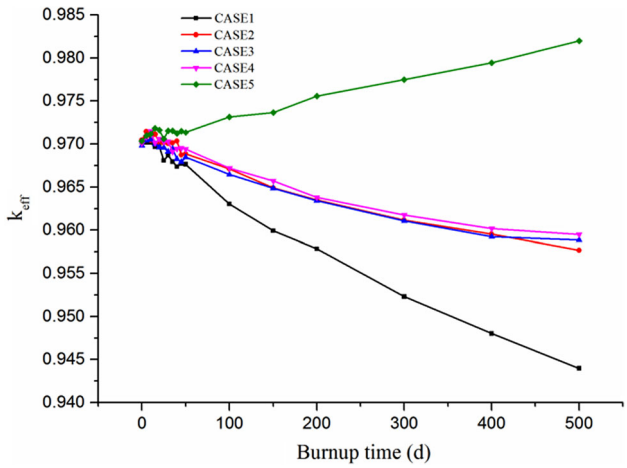

Fig. 3 Time evolution of the effective multiplication factor (k_{eff}) for different cases

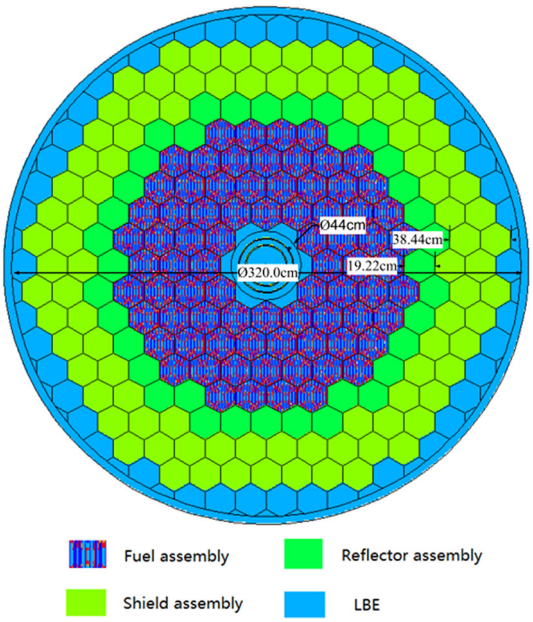

Fig. 4 (Color online) Radial profile of the ADS core

IHM over 3600 EFPDs are shown in Fig. 6b. In each fuel cycle, with the increase in burnup time, the total mass of MAs decreased, the total mass of Pu increased, and the mass percentage of Pu in HM increased continuously. The main reason for this is that ^{237}Np (in the MAs) generated ^{238}Pu, and the increase in all isotopes of Pu was greater than the loss. Refueling every 600 days was according to the fuel material provided in Table 5.

Variation of the core amplification factor over time is shown in Fig. 7. The core amplification factor is the weight of loss to fission per proton multiplied by $E_{\text{fission}}/E_{\text{beam}}$. In each fuel cycle, with increased burnup time, the core amplification factor continuously decreased. After replacement with new fuel, the core amplification factor increased significantly. The main reason for this was that in each fuel cycle, with the increase in time, part of the core fuel was consumed and the fuel available for fission reactions in the core decreased, which led to a decrease in the amplification factor. The maximum difference in the value of the core amplification factor during the whole cycle was 44.17%.

Variation of k_{eff} over time is shown in Fig. 8. k_{eff} decreased within each fuel cycle, but then increased when new fuel was introduced to the reactor. The main reason for the decreases in k_{eff} was that in each fuel cycle, increasing fuel consumption of the core resulted in a decrease in the number of newly generated neutrons in the core, which led to a decrease in the core k_{eff}. Variation of the maximum power density over time is shown in Fig. 9 and ranges from 256.00 to 274.14 W/cm^3, which is a relatively small change.

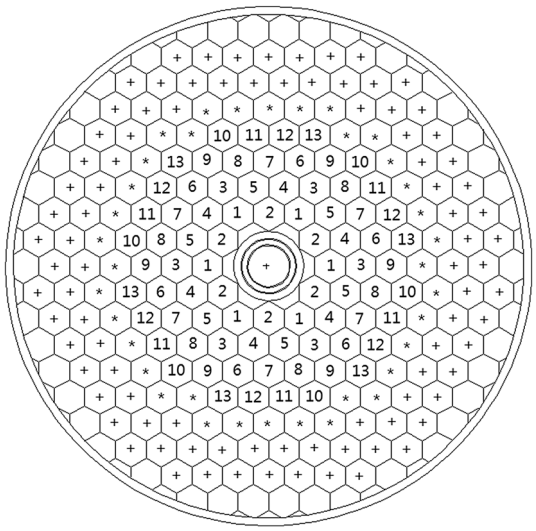

Fig. 5 Fuel assembly labeling scheme

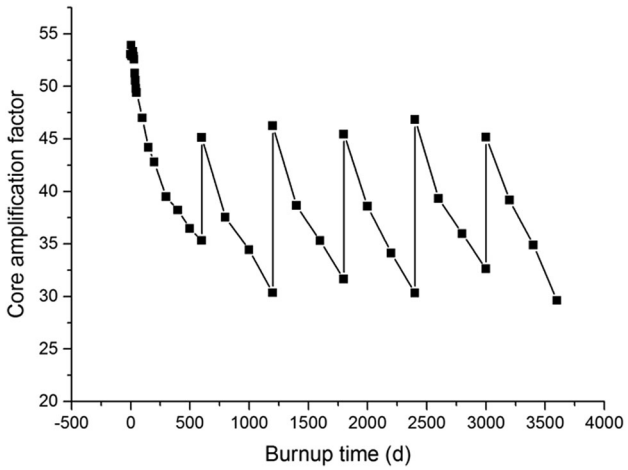

Fig. 7 Variation of core amplification factor over time

Table 5 Material number of fuel assemblies in different burnup cycles

Assembly number	0–600 days	600–1200 days	1200–1800 days	1800–2400 days	2400–3000 days	3000–3600 days
1	1001	1013	1019	1026	1032	1039
2	1002	1012	1018	1025	1031	1038
3	1003	1011	1017	1024	1030	1037
4	1004	1010	1016	1023	1029	1036
5	1005	1009	1015	1022	1028	1035
6	1006	1008	1014	1021	1027	1034
7	1007	1007	1020	1020	1033	1033
8	1008	1014	1021	1027	1034	1040
9	1009	1015	1022	1028	1035	1041
10	1010	1016	1023	1029	1036	1042
11	1011	1017	1024	1030	1037	1043
12	1012	1018	1025	1031	1038	1044
13	1013	1019	1026	1032	1039	1045

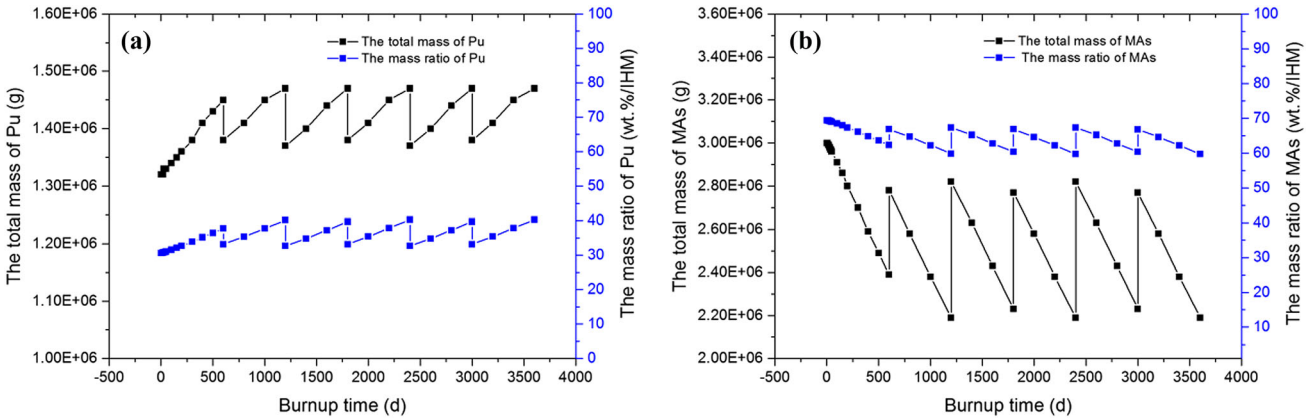

Fig. 6 Change in total mass and mass ratio of Pu (**a**) and MAs (**b**) in heavy metal

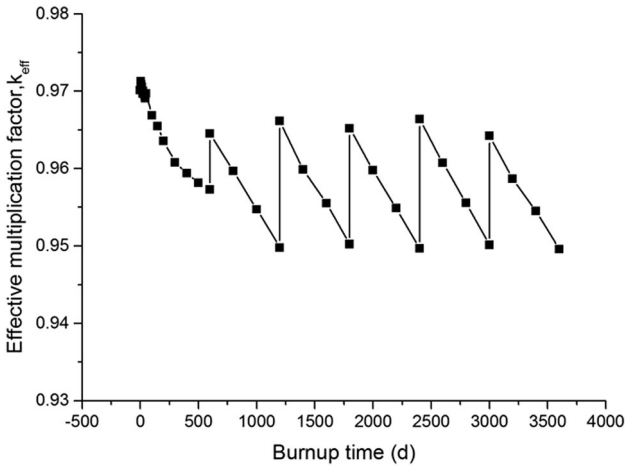

Fig. 8 Variation of effective multiplication factor over time

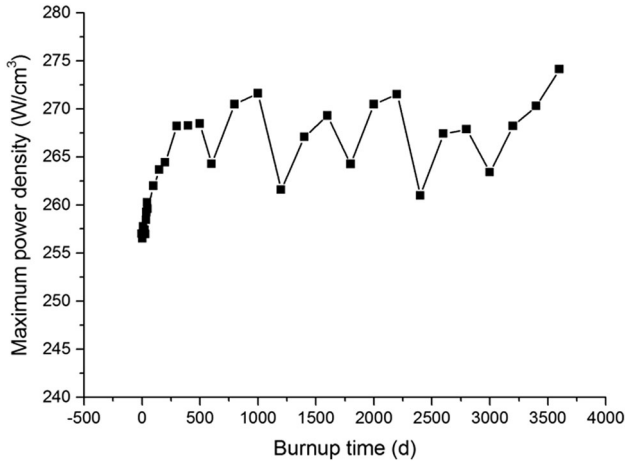

Fig. 9 Variation of core maximum power density over time

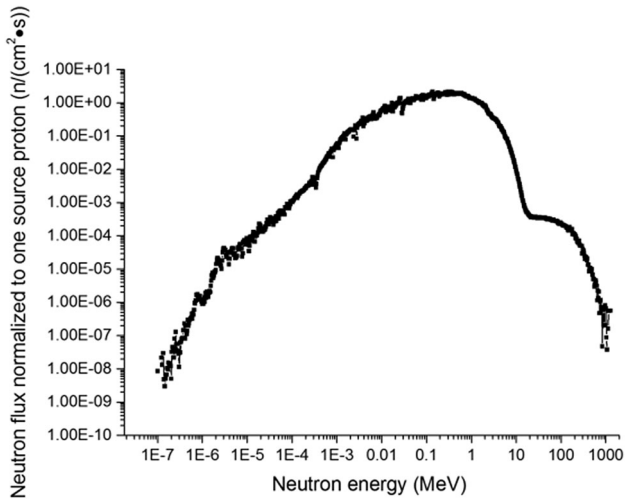

Fig. 10 Neutron energy spectrum in the initial ADS

Neutron energy spectrum in the initial ADS is shown in Fig. 10. The figure shows the ADS had a hard neutron energy spectrum, and the energy range of the neutron energy spectrum was wide. Changes in the mass percent of the major isotopes of Pu over time are shown in Fig. 11. Over each fuel cycle, the mass compositions of ^{239}Pu, ^{240}Pu and ^{241}Pu decreased, while those of ^{238}Pu and ^{242}Pu increased. After refueling, the mass compositions of ^{239}Pu, ^{240}Pu and ^{241}Pu increased, while those of ^{238}Pu and ^{242}Pu decreased. The main reason behind these observations is that in each fuel cycle, the total mass of Pu increased constantly, but the mass compositions of ^{239}Pu and ^{241}Pu decreased because the decrease in their masses was greater than their rate of generation. The total mass of ^{240}Pu in the core increased, but ^{240}Pu mass ratio decreased as the total Pu mass increased. Furthermore, a large amount of ^{238}Pu was transmuted from ^{238}Np through β decay, ^{239}Pu through (n,2n) reaction and ^{242}Cm through α decay. The disappearance rate of ^{238}Pu was far less than its rate of generation, which led to a relatively large increase in ^{238}Pu mass in the core, and a continuous increase in ^{238}Pu mass percent. The rate of disappearance of ^{242}Pu was less than its generation rate, and therefore, the core ^{242}Pu mass increased, and ^{242}Pu mass composition increased continuously. After refueling, Pu total mass decreased, and ^{239}Pu and ^{241}Pu mass increased, resulting in increased ^{239}Pu and ^{241}Pu mass ratios. The mass of ^{240}Pu decreased, but the reduction was not as great as the reduction of Pu total mass, so the mass ratio of ^{240}Pu increased. The mass of ^{238}Pu increased, Pu total mass decreased, and therefore, the mass composition of ^{238}Pu decreased. The mass of ^{242}Pu decreased, but its mass reduction was less than the mass of total Pu, resulting in the decrease in the mass composition of ^{242}Pu.

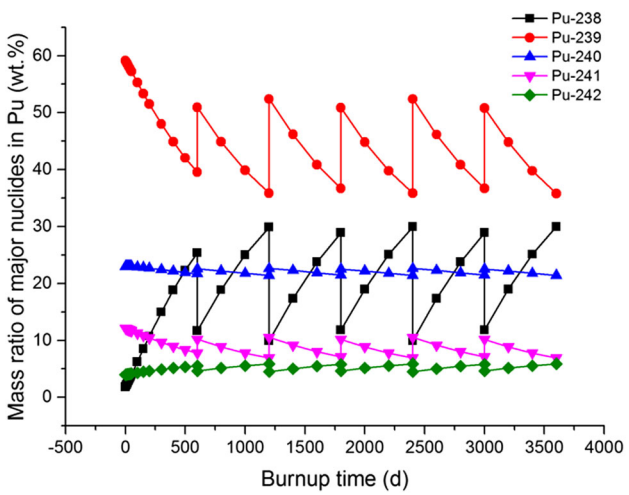

Fig. 11 (Color online) Changes in the mass ratio of the major isotopes of Pu

Changes in the mass percent of the major isotopes of MAs over time are shown in Fig. 12. Over each fuel cycle, the mass compositions of ^{237}Np and ^{241}Am decreased, while those of ^{242}Cm and ^{244}Cm increased and those of ^{241m}Am, ^{243}Am, ^{243}Cm and ^{245}Cm remained stable. After refueling, the mass compositions of ^{237}Np and ^{241}Am increased, while those of ^{242}Cm and ^{244}Cm decreased and those of ^{241m}Am, ^{243}Am, ^{243}Cm and ^{245}Cm remained stable. The main reason behind these observations is that in each fuel cycle, the total mass of the MAs decreased, and the decrease in ^{237}Np and ^{241}Am in their masses was greater than their rate of generation, and the reduction in their masses was greater than the decrease in the total mass of MA, and therefore, the mass compositions of ^{237}Np and ^{241}Am decreased. The total masses of ^{242}Cm and ^{244}Cm increased, and their mass compositions increased; the mass changes in ^{241m}Am, ^{243}Am, ^{243}Cm and ^{245}Cm were similar to that of the total mass of MAs, so their mass compositions did not change much in the entire burnup cycle. After refueling, MAs total mass increased, and ^{237}Np and ^{241}Am masses increased, which were larger than the increase in the total mass of MAs, resulting in increased ^{237}Np and ^{241}Am mass ratios. The masses of ^{242}Cm and ^{244}Cm decreased and MAs total mass increased, resulting in a decreased mass ratio of ^{242}Cm and ^{244}Cm in MAs.

Variation of the above-defined terms versus burnup time is shown in Fig. 13. Through 3600 EFPDs of the operation, the ΔM_{MA} was $-$ 3555.2 kg, $\Delta M_{MA\to Pu\to U}$ was 21.3 kg, $\Delta M_{MA\to Pu}$ was 1938.9 kg, and $\Delta M_{MA\to TRMA}$ was 5.8E $-$ 4 kg, which meant that ΔM_{MA} (EFF) was $-$ 1594.9 kg. Therefore, for the designed subcritical reactor, the specific ability for MA transmutation (SAMAT) was 1594.9/(0.8 $\times$ 3600/365) = 202.1 kg Gwt^{-1} a^{-1}.

The efficient transmutation supplier-to-burner support ratio (SBSR) is SAMAT/SAMAP. Therefore, for this ADS,

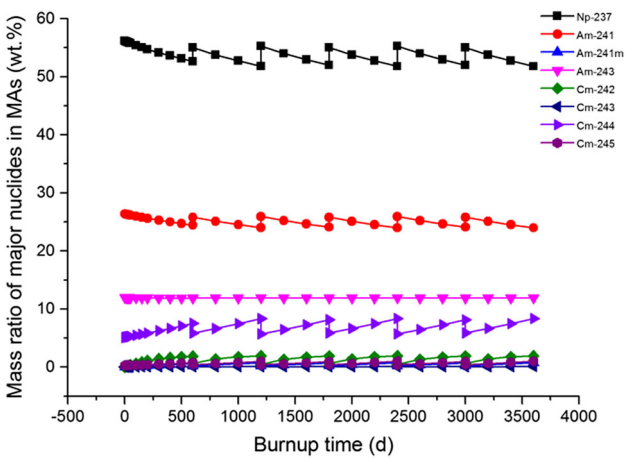

Fig. 12 (Color online) Changes in the mass ratio of the major isotopes of MAs

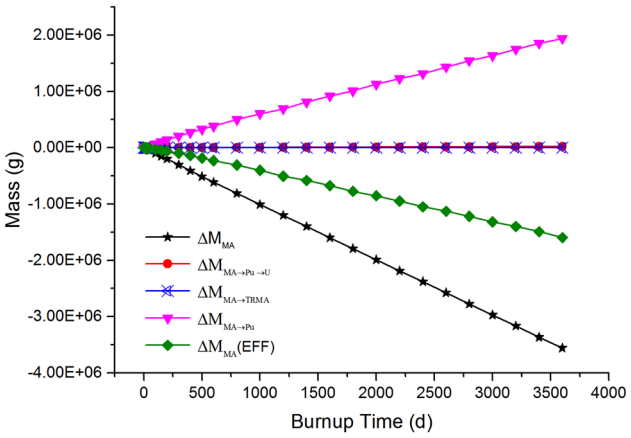

Fig. 13 ΔM_{MA}, $\Delta M_{MA\to Pu\to U}$, $\Delta M_{MA\to Pu}$, $\Delta M_{MA\to TRMA}$, ΔM_{MA} (EFF) with depletion time

the SBSR was 202.1/7.2 $\approx$ 28, demonstrating that this ADS was efficient at MA transmutation.

5 Conclusion

The physical study of a subcritical reactor of an ADS with a thermal power of 800 MW for the purposes of MA transmutation was undertaken. The initial loading of MAs was 3000 kg, and the fuel type was a mixture of mononitrides of MAs and Pu. Zirconium nitride (ZrN) was used in the fuel as an inert matrix. The analysis of the burnup characteristics was performed using the code COUPLE3.0. In order to ensure small changes in k_{eff} and safety of the subcritical core, refueling was undertaken every 600 days. Over each fuel cycle, the total mass of MAs decreased, the total mass of Pu increased, and the mass ratio of Pu increased constantly. After refueling, the total mass of MAs increased, the total mass of Pu decreased, and the corresponding mass composition of Pu decreased. In addition, the k_{eff} and core amplification factor decreased with burnup time, but both increased after refueling. The range of the maximum power density change was 256.00 $\sim$ 274.14 W/cm^3. The efficient transmutation supplier-to-burner support ratio (SBSR) of the selected subcritical core design was about 28, demonstrating that this ADS was efficient at MA transmutation.

References

1. Y. Zhou, China's spent nuclear fuel management: current practices and future strategies. Energy Policy **39**(7), 4360–4369 (2011). https://doi.org/10.1016/j.enpol.2011.01.055
2. D. Warin, Status of the French research program on partitioning and transmutation. J. Nucl. Sci. Technol. **44**(3), 410–414 (2007). https://doi.org/10.1080/18811248.2007.9711302

3. A. Gulevich, A. Kalugin, L. Ponomarev et al., Comparative study of ADS for minor actinides transmutation. Prog. Nucl. Energy **50**(2), 359–362 (2008). https://doi.org/10.1016/j.pnucene.2007.11.084
4. OECD/NEA, *Accelerator-Driven System (ADS) and Fast Reactors (FR) in Advanced Nuclear Fuel Cycles: A Comparative Study* (OECD/NEA, Paris, 2002). ISBN 92-64-18484-8
5. W.L. Zhan, H.S. Xu, Advanced fission energy program-ADS transmutation system. Bull. Chin. Acad. Sci. **27**(3), 375–381 (2012). https://doi.org/10.3969/j.issn.1000-3045.2012.03.017
6. H. Ait-Abderrahim, MYRRHA: a multipurpose accelerator driven system for research & development. Nucl. Instrum. Methods A **463**(3), 487–494 (2001). https://doi.org/10.1016/S0168-9002(01)00164-4
7. S.I. Tanaka, High intensity proton accelerator project in Japan (J-PARC). Radiat. Prot. Dosimetry. **115**(1–4), 33–43 (2005). https://doi.org/10.1093/rpd/nci139
8. T. Mukaiyama, H. Takano, T. Ogawa et al., Partitioning and transmutation studies at JAERI both under OMEGA program and high-intensity proton accelerator project ☆. Prog. Nucl. Energy **40**(3–4), 403–413 (2002). https://doi.org/10.1016/S0149-1970(02)00032-X
9. M. Viala, M. Salvatores, H. Mouney, The SPIN program-assets and prospects, in Paper Presented at Proceedings of the International Conference on Future Nuclear System (Global'97), Yokohama, Japan, 5–10 October, 1997
10. K. Tsujimoto, T. Sasa, K. Nishihara et al., Neutronics design for lead-bismuth cooled accelerator-driven system for transmutation of minor actinide. J. Nucl. Sci. Technol. **41**(1), 21–36 (2004). https://doi.org/10.1080/18811248.2004.9715454
11. S. Ishida, H. Sekimoto, Finding the best fuel assemblies shuffling scheme of ADS for MA transmutation using dynamic programming. Nucl. Eng. Des. **240**(10), 3645–3653 (2010). https://doi.org/10.1016/j.nucengdes.2010.07.008
12. L. Zhang, Y.W. Yang, Y.G. Fu et al., Development and validation of the code COUPLE3.0 for the coupled analysis of neutron transport and burnup in ADS. Nucl. Sci. Technol. **29**(9), 124 (2018). https://doi.org/10.1007/s41365-018-0471-4
13. D.B. Pelowitz, *MCNPX User's Manual, Version 2.7.0* (Los Alamos National Laboratory, Los Alamos, 2011)
14. A.G. Groff, ORIGEN2: A Revised and Updated Version of the Oak Ridge Isotope Generation and Depletion Code. ORNL-5621 (1980)
15. A. Talamo, W. Ji, J. Centar et al., Comparison of MCB and MONTEBURNS Monte Carlo burnup codes on a one-pass deep burn. Ann. Nucl. Energy **33**(14–15), 1176–1188 (2006). https://doi.org/10.1016/j.anucene.2006.08.006
16. A. Stankovskiy, G.V.D. Eynde, P. Baeten, et al., ALEPH2—a general purpose Monte Carlo depletion code, in Paper Presented at PHYSOR 2012: Conference on Advances in Reactor Physics—Linking Research, Industry, and Education. Knoxville, Tennessee, USA, 15–20 April, 2012
17. Y. Arai, M. Akabori, K. Minato, Progress of nitride fuel cycle research for transmutation of minor actinides (2007)
18. International Atomic Energy Agency. https://www-nds.iaea.org. Accessed 13 July 2018
19. T. Mukaiyama, H. Yoshida, T. Ogawa, Minor actinide transmutation in fission reactors and fuel cycle considerations. IAEA-TECDOC-693 (IAEA, Vinenna, 1993)
20. N.Z. Zainuddin, G.T. Parks, E. Shwageraus, The factors affecting MTC of thorium–plutonium-fuelled PWRs. Ann. Nucl. Energy **98**, 132–143 (2016). https://doi.org/10.1016/j.anucene.2016.07.034